ELSEVIER

Cross-link Profile of Bone Collagen Correlates With Structural Organization of Trabeculae

X. BANSE,[1] J. P. DEVOGELAER,[1] A. LAFOSSE,[1] T. J. SIMS,[3] M. GRYNPAS,[2] and A. J. BAILEY[3]

[1]Orthopaedic Research Laboratory and Arthritis Unit, Université Catholique de Louvain, Brussels, Belgium
[2]Samuel Lunenfeld Research Institute, Mount Sinai Hospital, Toronto, ON, Canada
[3]Collagen Research Group, Division of Molecular and Cellular Biology, University of Bristol, Langford, Bristol, UK

Little is known regarding the mechanisms that govern the structural organization of cancellous bone. In this study, we compare the nature of the collagen in vertebral cancellous bone with the structural organization of its trabecular network. Cylindrical specimens of cancellous bone from vertebrae were obtained from nine autopsy subjects (ages 46–88). In each subject, eight pairs of corresponding samples were obtained from three levels in the spine and three areas within the vertebral body, leading to a total of 68 pairs of samples. The cylinders from one side were used for morphometry and the classical morphometrical parameters were obtained (BV/TV, bone volume fraction; Tb.Th, trabecular thickness; Tb.N, number; Tb.Sp, trabecular spacing) and strut analysis (TSL, total strut length; Nd, number of nodes; Fe, number of free-ends). The amount of osteoid bone was also quantified. The cylinders from the other side were powdered and used for collagen assessment, including the amount of collagen (% w/w), and its content in immature cross-links; such as hydroxylysinonorleucine (mol/mol of collagen) and dihydroxylysinornorleucine, as well as stable mature cross-links, such as hydroxylysylpyridinoline (HP), lysylpyridinoline (LP), and the pyrrole cross-links. A random regression model was used to explore the correlations. None of the biochemical parameters correlated with the BV/TV except the ratio between immature and mature cross-links ($\eta^2 = 0.34$, $p < 0.05$). There was no relationship between the amount of osteoid bone and the cross-link profile. However, the concentration of pyrrole and HP cross-links in the bone samples correlated with the structural organization of its trabeculae, but in an opposite direction. Hence, the pyrrole/HP ratio was a good predictor of Tb.Th, Tb.N, Tb.Sp, and TSL ($\eta^2 > 0.65$ and $p < 0.01$) as well as Fe and star marrow space ($\eta^2 > 0.45$ and $p < 0.05$). The cylinders from subjects with high pyrrole or low HP in their bone collagen had a relatively thick and simple structure. Those with low pyrrole and high HP had relatively thin trabeculae that were more numerous and spread over a complex network. The relative concentrations of the pyrrole and pyridinoline cross-links appear to reflect the structural organization of the trabeculae. (Bone 31: 70–76; 2002) © 2002 by Elsevier Science Inc. All rights reserved.

Address for correspondence and reprints: Dr. Xavier Banse, Université Catholique de Louvain, Orthopaedic Research Laboratory, Tour Pasteur 5388, Avenue E. Mounier 53, B-1200 Bruxelles, Belgium. E-mail: xavier.banse@orto.ucl.ac.be

Introduction

Nature of the Bone Matrix

Bone is a highly specialized connective tissue. It can be viewed as a dense packing of collagen fibers in which large amounts of solid mineral crystals are deposited. The relative amounts and properties of both the mineral and the organic matrix influence the behavior of the structure. Type I collagen is the principal constituent of the organic matrix, representing 90% of its weight. The primary sequence of the molecule is identical in bones and elsewhere in the body, but posttranscriptional modifications vary with the type of tissue.[19,29] The formation of specific cross-links is controlled enzymatically both through the hydroxylation of specific lysine residues and their subsequent enzymatic conversion to aldehydes. When compared with other tissues (tendon, fascia, skin), bone collagen has a specific cross-link profile due to the high degree of lysyl hydroxylation in the telopeptide, whereas that in the triple helix is low. The predominant cross-link in young bone is the divalent hydroxylysino-*keto*-norleucine which is converted, with increasing age, to the trivalent hydroxylysyl- and lysylpyridinolines and pyrroles (**Figure 1**).[10,20] The immature divalent cross-links are still present to a limited extent in mature bone due to the relatively high turnover of bone collagen. The cross-link profile was found not to vary with age in adults,[2] but seems to vary among patients.[10] Overall, the fibrillogenesis and maturation of the collagen is most certainly controlled by the posttranslational modification of the molecule resulting in the formation of a specific cross-link profile.[29]

Structural Organization of Vertebral Cancellous Bone

Vertebral cancellous bone has an especially low bone volume fraction (BV/TV): only 7%–14% of the total volume is occupied by bone tissue, the rest being marrow. With such a small amount of material, an optimal structural organization (called microarchitecture) is of primary importance.[18] It may affect (by itself) both static and dynamic mechanical properties of the cancellous bone. Patients with osteoporotic vertebral crush fractures have been reported to have a poor, disconnected cancellous bone structure compared with controls matched for bone density.[12] In vitro testing of samples has also led to similar findings.[16] In addition, some types of structures, for example those with relatively thin trabeculae, may be more sensitive to normal remodeling and,
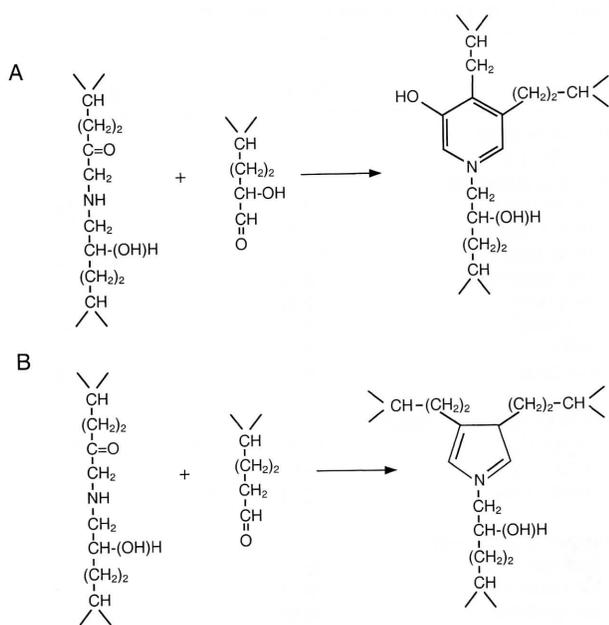
Figure 1. Formation of the pyridinoline and pyrrole cross-links. (A) A hydroxylysyl aldehyde residue reacts with a lysino-*keto*-norleucine cross-link to form the trivalent lysylpyridinoline (LP) or with the hydroxylysino-*keto*-norleucine to form a hydroxylysylpyridinoline (HP). Note that the only difference is the OH group in the initial bivalent cross-link. (B) If a lysyl aldehyde reacts with the same immature cross-link it forms the lysyl and hydroxylysylpyrrole cross-link. The structure proposed by Kuypers et al.[21] is presented. Whether a pyrrole or a pyridinoline is formed depends on the hydroxylation (or not) of the added lysyl aldehyde from the telopeptide.

especially, to the acceleration of turnover occurring with menopause, disease, or drugs. Recently, we have shown that the structural organization of trabeculae in vertebral cancellous bone was patient-specific.[5] The complex microarchitecture of the trabeculae, or at least its persistence, ultimately depends on the location and shape of the resorption lacunae and on the ability of the osteoblasts to refill these cavities. For example, deleterious plate perforations or bar disconnections may occur during the resorption phase of the remodeling cycle, resulting in a definitive change in the structure.[23]

To date, there has been no study comparing the collagen cross-link profile of cancellous bone with histomorphometrical data. Correlating the nature of the bone material deposited with the final structure obtained may help in understanding the biology of bone remodeling. In this study, we had the opportunity to combine both types of investigation and address the following questions:

1. Is there a specific cross-link profile associated with low bone density?
2. Is there a relationship between the "maturity" of the cross-links and the indices of new bone formation (that measure the amount of bone tissue that is not yet mineralized)?
3. Is there a correlation between the structural organization of the trabeculae (estimated by the morphometrical parameters) and the chemical nature of its organic matrix (estimated by its cross-link content)?

Materials and Methods

Sample Collection

The specimens came from nine autopsy subjects (three women
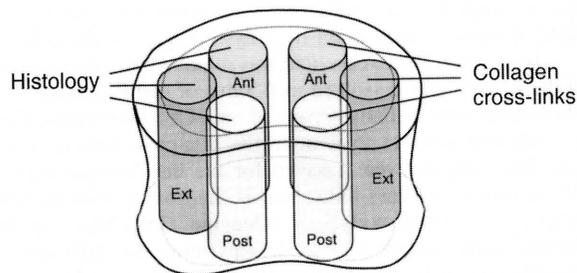
Figure 2. Locations of coring in a vertebral body. A thoracolumbar or lumbar vertebral body is illustrated (viewed from the back). Six cylinders were extracted from that vertebra. Samples came from the anterior (Ant), posterior (Post), or external (Ext) area and comprised three pairs. The samples from one side were used for the collagen analysis, whereas samples from the other side were used for the histology. Overall, 68 pairs of samples were analyzed.

and six men, ages 44–88) with no disease known to affect bone.[5] Three vertebral bodies (one thoracic at T-9, one thoracolumbar at T-12–L-1, and one lumbar at L-4) were obtained from each of them. Eight pairs of cylindrical samples (8.2 mm diameter) were vertically cored from each subject: two in the T-9 vertebral body, three in the T-12 or L-1, and three in the L-4, with each cylinder from one side having its symmetrically matched control from the other side (**Figure 2**). In one T-12 specimen the external sample was not obtained and, in another subject, the L-4 vertebral body was discarded because of degenerative disk lesions, leaving 68 pairs of samples for the study: 68 cylinders on one side used for histomorphometry, and 68 paired cylinders from the other side used for biochemistry.

Biochemical Analysis

The endplates of the 68 samples for the cross-link analysis were removed, leaving only pure cancellous bone for biochemistry. The samples were washed thoroughly under a jet of de-ionized water to remove bone marrow and blood cells, defatted in a 1:1 (v/v) chloroform-methanol solution, rinsed with methanol then with de-ionized water, and finally freeze-dried.

Collagen Determination

The amount of collagen was determined by hydroxyproline assay of an aliquot of the acid hydrolysate (6 mol/L HCl, 110°C, 16 h) using a continuous-flow AutoAnalyzer (Burkard Scientific, Uxbridge, UK) based on the method of Grant.[13] The accuracy of the method was checked occasionally by the determination of hydroxyproline on the amino acid analyzer. Collagen content was calculated on the dry weight of the bone assuming 14% hydroxyproline in type I collagen. The resulting data were then used to calculate the cross-link values as moles per mole of collagen.

Intermolecular Cross-links

The intermediate cross-links of the newly synthesized collagen were stabilized by borohydride reduction prior to acid hydrolysis, and both reduced and mature cross-links were determined after acid hydrolysis on a modified amino acid analyzer as previously described in detail.[32,33] Briefly, the bone samples were homogenized to avoid any possibility of differences due to thickness of the bone, suspended in phosphate-buffered saline, and reduced with potassium borohydride. The samples were washed, freeze-

dried, reweighed, and hydrolyzed in 6 mol/L HCl for 24 h at 110°C in screw-topped glass hydrolysis tubes (Medline Scientific, Oxon, UK). The excess acid was removed by freeze-drying, and the residue was dissolved in 0.5 mL of distilled water. The hydrolysates were initially separated on a CF1 (Whatman, Kent, UK) cellulose column to remove the non-cross-linking amino acids. The samples were assayed for the borohydride reduced form of immature cross-links; that is, hydroxylysinonorleucine (HLNL) and dihydroxylysinornorleucine (DHLNL) together with the stable mature hydroxylysylpyridinoline (HP) and lysylpyridinoline (LP) cross-links, using a modified gradient on an amino acid analyzer (Alpha Plus, Pharmacia, Loughborough, UK). The location of the cross-links on the analyzer had been confirmed previously with samples of authentic cross-links prepared in the laboratory. Quantification of the cross-links was achieved using ninhydrin color reaction and their known leucine equivalents.

Pyrrolic Cross-link

Bone matrix (100 mg) was dispensed into polypropylene tubes (Sarstedt, Leicester, UK) and initially decalcified by suspension (20 mg/mL) in 0.5 mol/L tetrasodium ethylene-diamine tetraacetic acid (EDTA), pH 7.5, for 3 days at 4°C. The EDTA was decanted after centrifugation (10,000 rpm) and the decalcified matrix was resuspended in distilled water, shaken, and subsequently centrifuged (10,000 rpm). After repeating this wash step, 1200 μL of 0.1 mol/L 3-[N-tris(hydroxymethyl)methylamino]-2-hydroxy-propanesulphonic acid (TAPSO), pH 8.2, was dispensed into each tube and the sample heat denatured at 100°C for 30 min and then allowed to cool to 37°C. Samples were then treated with 1000 units of trypsin (TPCK-treated) dispensed from a trypsin stock (5000 U/mL TAPSO buffer) and left to digest by shaking gently for 18 h at 37°C. The pyrrole content of the digest was assayed by reaction with *p*-dimethylaminobenzaldehyde (DAB) using a microtiter plate format[32] (Micro Test III Flexible Plate, Becton Dickinson). Quantification was facilitated by the inclusion of a 1-methylpyrrole (Aldrich, Dorset, UK) standard (range 1–10 mmol/L) prepared from a stock solution (50 mmol/L in ethanol). A 50 μL aliquot was removed for total collagen content by the hydroxyproline assay just described. A further 250 μL of each sample was combined with 50 μL of DAB (11.4% w/v in 60% perchloric acid). Within 15 min of adding the DAB, all samples were filtered, employing a 0.2 μm syringe filter (13 mm, HPLC Technology, Macclesfield, UK) and 180 μL of the sample was dispensed into a 96 well microtiter plate and read at 570 nm using a microtiter plate reader (Labsystems Multiskan MCC 340). The pyrrole content of the bone digests was calculated based on the extinction coefficient of 25,000 for 1-methylpyrrole[31] and expressed as moles of pyrrole per mole of collagen based on the hydroxyproline assay.

The ratio between the immature and mature cross-links (immature/mature ratio) was calculated as: (DHLNL + HLNL)/(pyrrole + HP + LP). As an additional parameter, we also calculated the ratio between pyrrole and HP cross-links.

Histomorphometry

The 68 samples dedicated to histology were fixed and embedded in Spurr resin using a standard protocol.[30] The plastic blocks containing the whole cylindrical specimen were then cut at four levels to cover its volume from the top to the bottom. Thin sections (5 μm) were obtained. One was stained with Von Kossa, which visualizes the mineral in black; another was stained with Goldner trichrome, which shows the mineralized tissue in green and the osteoid nonmineralized tissue in red.

Table 1. Mean values observed for the 68 cylindrical samples

Parameter	Mean	SD	Correlation with BV/TV (η^2)
Amount of bone			
BV/TV (%)	7.9	2.3	
Structural parameter			
Tb.Th (μm)	84	13	0.75[b]
Tb.N (-/mm^2)	0.93	0.18	0.87[b]
Tb.Sp (μm)	1050	231	0.84[b]
TSL (mm/mm^2)	0.78	0.17	0.86[b]
Nd (-/mm^2)	0.81	0.24	0.87[b]
Fe (-/mm^2)	2.5	0.4	0.05
Nd/Fe (-)	0.33	0.08	0.91[b]
Star (mm^2)	6.9	2.2	0.82[b]
New bone formation indices			
OS/BS (%)	16.5	11.9	0.03
O.Th (μm)	6.9	0.9	0.44[a]
OV/BV (%)	2.71	2.17	0.04
Collagen biochemistry			
Collagen (%)	26	2	
HP (mol/mol)	0.13	0.04	
LP (mol/mol)	0.071	0.030	
Pyrrole (mol/mol)	0.094	0.016	
Pyrrole/HP (-)	0.83	0.39	
DHLNL (mol/mol)	0.120	0.052	
HLNL (mol/mol)	0.076	0.023	
Immature/mature (-)	0.69	0.22	

Mean and standard deviation for all the parameters included in the study. The link or correlation between the BV/TV and the other morphometrical parameters is estimated by eta-squared (η^2).
KEY: BV/TV, trabecular bone volume fraction; Tb.Th, trabecular thickness; Tb.N, trabecular number; Tb.Sp, trabecular spacing; TSL, total strut length (on the skeletonized image); Nd, nodes or multiple point; Fe, free-ends or disconnections; Nd/Fe, ratio between nodes and free-ends (index of connectivity); Star, star surface; OS/BS, osteoid; OV/BV, osteoid volume; O.Th, osteoid thickness; HP, hydroxylyslpyridinoline; LP, lysylpyridinoline; DHLNL, dihydroxylycinonorleucine; HLNL, hydroxylysylpyridinoline.
[a]$p < 0.05$; [b]$p < 0.001$.

Von Kossa: Structural Parameters

A digital image of each Von Kossa thin section was obtained (resolution 1 pixel = 10 μm) and analyzed as previously described.[4] The morphological classical parameters were measured according to ASBMR standards.[24] These included trabecular volume fraction (BV/TV, %), trabecular number (Tb.N, mm^{-2}), trabecular thickness (Tb.Th, μm), and trabecular spacing (Tb.Sp, μm). The binary images were then skeletonized and pruned to quantify total strut lengths (TSL, mm/mm^2). The multiple point or nodes (Nd, mm^{-2}) as well as the free-ends (Fe, mm^{-2}) were then identified on this skeleton.[7] The ratio of the number of nodes and number of free-ends (Nd/Fe, −) was also calculated and considered as an index of connectivity. Finally, we measured the star marrow space (Star, mm^2).[12,35]

Goldner Trichrome: New Bone Formation Indices

For detection of osteoid layers a higher magnification is required. Consequently, each slice was scanned to obtain 40 contiguous pictures (covering 60% of the section, pixel size 1 μm). As for the Von Kossa, the image analysis was carried out using a Quantimet 500IW running a homemade macro under QwinPro (Leica imaging system, Cambridge, UK). A constant color threshold (on the RGB) was used to differentiate the tissues.

Table 2. Correlation between histomorphometry and biochemistry (η^2 values)

Histomorphometry	Collagen biochemical parameter							
	Collagen (%)	HP (mol/ mol)	LP (mol/ mol)	Pyrrole (mol/mol)	Pyrrole/HP (-)	DHLNL (mol/mol)	HLNL (mol/mol)	Immature/ mature (-)
Amount of bone								
BVTV (%)	0.11	0.03	0.05	0.00	0.00	0.08	0.11	0.34[a] +
Structural parameter								
Tb.Th (μm)[d]	0.19	0.43[a] −	0.14	0.62[c] +	0.74[c] +	0.09	0.25	0.03
Tb.N (-/mm^2)[d]	0.12	0.43[a] +	0.08	0.56[b] −	0.68[c] −	0.08	0.20	0.02
Tb.Sp (μm)[d]	0.10	0.43[a] −	0.09	0.55[b] +	0.66[c] +	0.10	0.14	0.01
TSL (mm/mm^2)[d]	0.07	0.49[b] +	0.09	0.53[b] −	0.67[c] −	0.17	0.19	0.05
Nd (-mm^2)[d]	0.04	0.11	0.00	0.51[b] −	0.31	0.00	0.16	0.01
Fe (-/mm^2)	0.17	0.13	0.03	0.50[b] −	0.45[a] −	0.03	0.16	0.00
Nd/Fe (-)[d]	0.20	0.03	0.10	0.04	0.09	0.09	0.02	0.11
Star (mm^2)[d]	0.08	0.42[a] −	0.11	0.43[b] +	0.58[c] +	0.06	0.14	0.00
New bone formation indices								
OS/BS (%)	0.41	0.14	0.02	0.09	0.09	0.04	0.06	0.00
O.Th (μm)[d]	0.00	0.00	0.03	0.05	0.05	0.04	0.04	0.06
OV/BV (%)	0.02	0.18	0.02	0.15	0.15	0.03	0.09	0.00

The η^2 value is an estimate of the part of the total variability (in the morphometrical parameter) explained by the biochemical parameter. Significant correlations were found between the cross-links and multiple structural parameters.
KEY: +, positive correlation; −, negative correlation. See Table 1 and *Results* for other abbreviations.
[a]Uncorrected $p < 0.05$.
[b]Uncorrected $p < 0.02$ and corrected $p < 0.10$.
[c]Uncorrected $p < 0.01$ and corrected $p < 0.05$.
[d]BV/TV was introduced first into the model, meaning the η^2 value is rather a partial correlation coefficient.

About 10,000 images were processed. The total bone and osteoid surfaces and perimeters were summed for a given sample to compute the following new bone formation parameters: osteoid volume (OV/BV, %), osteoid thickness (O.Th, μm) and osteoid surface (OS/BS, %).

Data Processing and Statistical Analysis

SPSS version 10.0 (SPSS, Inc., Chicago, IL) was used for data processing and statistical analysis. A total of 12 histological parameters (9 structural and 3 osteoid) describing 68 cylinders were compared with 8 biochemical parameters describing the 68 corresponding cylinders.

Relationships between variables were investigated using a random effects regression model. The morphometrical parameter was the dependent variable (or outcome). Introducing the name of the subject as having a random effect accounted for the repeated nature of the data (8 cylinders assessed in each subject) and allows for testing the significance of the variations among subjects. The biochemical parameter was introduced as a covariable in the model. When a morphometrical parameter was strongly linked to the BV/TV (as was the case for most of them; see **Table 1**), two covariables were used in the model: BV/TV was introduced first, followed by the biochemical parameter. Using this procedure, the model explored the relationship between the biochemical parameter and the variance of the morphometrical parameter that was not explained by the BV/TV.

For the correlation between variables, eta-squared (η^2) was calculated. η^2 estimates the part of the total variability of the dependent variable that can be explained by a given covariable. Such a parameter is analog to the correlation coefficient (r) in classical regression. As multiple comparisons were performed (see **Table 2**), a Bonferroni correction to the p value was applied. We report the corrected and uncorrected p values. The r values were also calculated but were not used to decide whether the correlation was significant or not.

Furthermore, to illustrate this "purely morphometrical" infor-

mation,[4] we used the residues of the regression between the parameter (e.g., the Tb.Th or Tb.Sp) and the BV/TV as raw data (indicated with an asterisk [Tb.Th* or TSL*] in Figures 4 and 5). For example, a value of 15 μm for Tb.Th* means that the trabeculae of that given sample were 15 μm thicker than expected knowing the BV/TV.

Results

Mean Values

Our data confirm the low density of the samples, with only 8% of the volume being occupied by bone. The trabeculae were thin (84 μm) and widely spaced (>1000 μm). The nodes (Nd) were relatively rare, with less than 1 node/mm^2 and about three free-ends (Fe, or disconnection) for a node. All these raw parameters (except the Fe) were highly correlated with BV/TV. We found unmineralized osteoid bone in all the samples. The cross-link profile was typical of bone collagen, with immature cross-links (DHLNL and HLNL), and mature lysylpyridinoline (LP) and pyrrole found in significant amounts (Table 1).

Density and Cross-links

Although the sampling covered a wide range of density (BV/TV range 4.6%–15.6%), none of the collagen properties correlated with BV/TV, except for a mild correlation ($\eta^2 = 0.34$, $p < 0.05$, and $r = 0.39$) between the immature/mature ratio and the BV/TV (Table 2).

Osteoid and Cross-links

None of the biochemical parameters correlated with either osteoid volume (OV/BV), osteoid thickness (O.Th), or osteoid surface (OS/BS). More specifically, there were no more immature cross-links (DHLNL or HLNL, immature/mature ratio) when the new synthesis rate was high.

Subject No 8:
Low pyrrole, high HP, thin structure

Subject No 7:
High pyrrole, low HP, thick structure
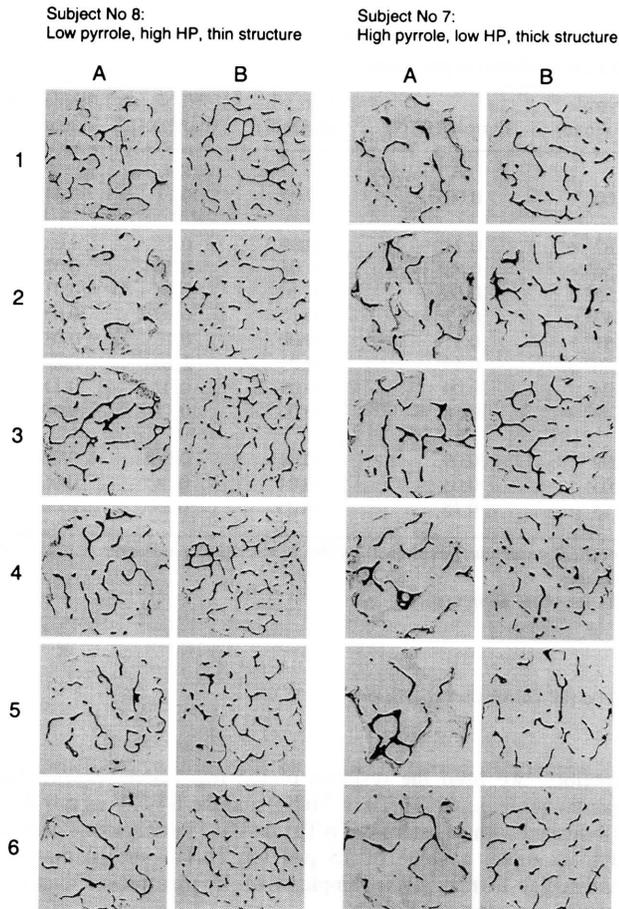
Figure 3. Thin sections (5 μm) of the vertebral cancellous bone exhibiting two different structural organizations of the trabeculae. Twelve slices (Von Kossa staining, width of a square image is 8.2 mm) from identical anatomical locations but from two different subjects (subject 8 [left] and subject 7 [right]) are compared. In one column, slices come from the center of the vertebral body (A) and in the other column they come from closer to the endplate (B). Each row corresponds to a given cylinder: 1, 2, and 3 are anterior, posterior, and external cylinders from the thoracolumbar (L-1) vertebra, respectively; and 4, 5, and 6 are the anterior, posterior, and external cylinders from the lumbar (L-4) vertebra, respectively. Both subjects had essentially the same BV/TV (7.38% and 7.95%). The structural organization of the trabeculae was not identical: Tb.Th was 81 μm on the left and 100 μm on the right; Tb.Sp was 1000 μm on the left and 1250 μm on the right; TSL was 0.82 mm/mm^2 on the left and 0.66 on the right; and Fe was 2.41/mm^2 on the left and 1.84 on the right. This is visible on the image. The structural organization of the trabeculae of subject 8 was more complex and the elements were thinner than subject 7. The first had less pyrrole and more HP than the second.

Structure and Cross-links

Samples with a high pyrrole concentration had relatively thick trabeculae (Tb.Th: $\eta^2 = 0.62$, $p < 0.01$, and $r = 0.67$; see **Figures 3, 4A**, and **5**), that were less numerous (Tb.N: $\eta^2 = 0.56$, $p < 0.02$, and $r = -0.59$) and more widely spaced (Tb.Sp: $\eta^2 = 0.55$, $p < 0.02$, and $r = 0.59$). Furthermore, the trabecular network was significantly less complex, spreading over a decreased length (TSL: $\eta^2 = 0.53$, $p < 0.02$, and $r = -0.55$) with fewer nodes (Nd: $\eta^2 = 0.53$, $p < 0.02$, and $r = -0.55$) and fewer disconnections (Fe: $\eta^2 = 0.50$, $p < 0.02$, and $r = -0.56$; see **Figure 4B**). Finally, the star marrow space was smaller when the pyrrole values were high (Star: $\eta^2 = 0.43$ and $r = 0.56$). All
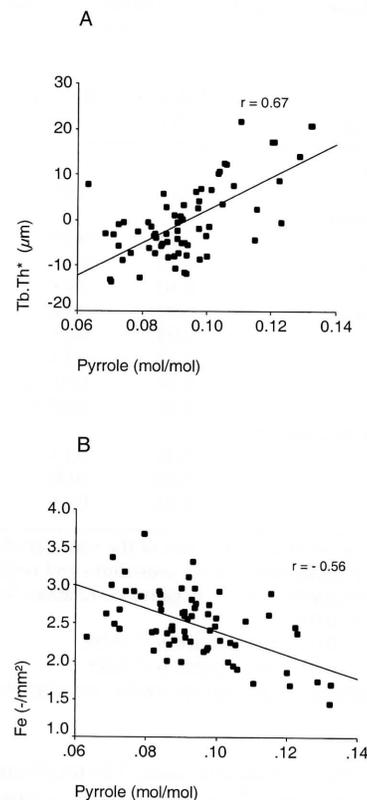
Figure 4. Correlation between the concentration of pyrrole cross-link and the structure (n = 68). After correction for the (dominant) BV/TV influence, the trabecular thickness (Tb.Th*, μm) of a given cylinder correlated positively with the concentration of pyrrole. The number of free-ends (Fe, -/mm^2) correlated negatively with the concentration of pyrrole.

these correlations are consistent with the concept that high pyrrole content results in a thick, simple, and disconnected structure.

Opposite relationships were noted for HP concentration. A high concentration of HP was associated with a thinner and more complex structure (for details see Table 2). It should be noted that the concentration of HP correlated negatively with concentration of pyrrole ($r = -0.33$). We investigated the combination of these two predictors (HP and pyrrole). First, we built a model that included both predictors in variable order: (i) first HP, then pyrrole or (ii) first pyrrole, then HP. In both cases, it appeared that the addition of a second biochemical parameter (either HP or pyrrole) added some independent explanatory value ($p < 0.05$). Because the relationship was in the opposite direction we computed the ratio between both of them (pyrrole/HP). For the ratio the correlation was even higher. A high ratio was associated with a thicker structure (i.e., Tb.Th: $\eta^2 = 0.74$, $p < 0.01$, and $r = 0.75$).

After the Bonferroni correction for multiple comparisons, only the uncorrected p values <0.01 remained significant (corrected p values <0.05). After correction, the other p values indicated a trend ($p < 0.10$).

Subject-specific Data

All investigated parameters (listed in Table 1) were strongly subject-specific as a significant between-subject variance ($p <$
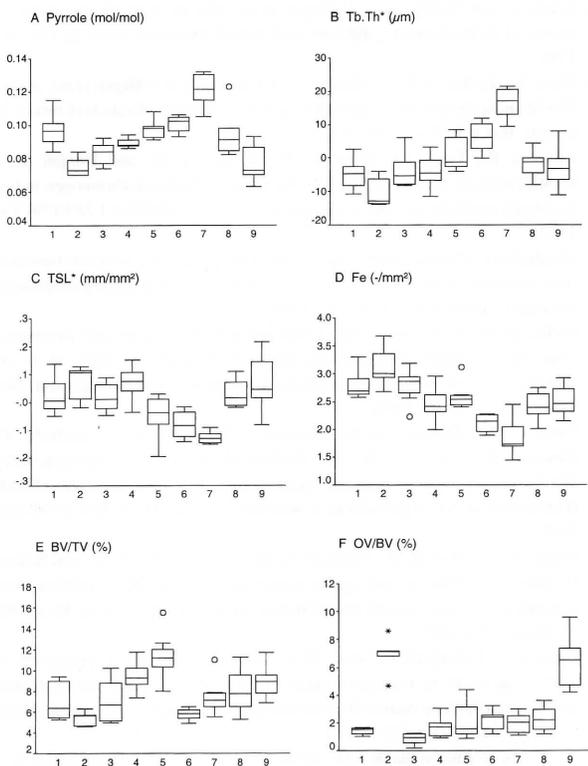
Figure 5. Boxplot charts of some parameters used in this study according to the subject from whom the samples were obtained (numbers 1–9 on the Category axis). Most of the parameters were patient-specific ($p <$ 0.001). Different subjects had different amounts of pyrrole (Pyrrole, mol/mol) (A), and different microarchitecture as illustrated here by the values of corrected trabecular thickness (Tb.Th*, μm) (B), corrected total strut length (TSL*, mm/mm^2) (C), and number of free-ends (Fe, -/mm^2) (D). The density or bone volume fraction (BV/TV, %) (E) and osteoid volume (OV/BV, %) (F) also varied between subjects. Note that pyrrole and Tb.Th* charts have the same appearance. Fe and TSL charts present a mirror image of the pyrrole chart. BV/TV or OV/TV are difficult to compare with any other parameters.

0.001) was detected in the random regression model (Figure 5). The only exception was HLNL concentration, which did not vary significantly among the nine subjects. When the Von Kossa-stained thin sections of two subjects with the same BV/TV were compared, differences in the structural organization of the trabeculae appeared (Figure 3).

Discussion

The present observations indicate a relationship between the nature of the bone collagenous matrix, in particular the concentration of the pyrrole and HP cross-links, and the structural organization of the trabeculae. A high pyrrole/HP ratio content was found to be correlated with a thick, simple, apparently disconnected structure, whereas a low pyrrole/HP ratio reflected a thin, complex, and more connected structure (Figure 3). In contrast, the properties of the collagenous matrix did not correlate with the density (BV/TV) nor with the new bone formation indices. The results were analyzed in detail using an adapted statistical model (the random regression model) that takes into account the repeated nature of the data and allows for testing the significance of the correlations between the parameters.[11] After Bonferroni correction for multiple comparisons,[28] a substantial

proportion of these correlations remained significant (see Table 2). The random regression model and the simple direct correlations (n = 68) were consistent as they both pointed out the same pairs of variables.

The absolute values of the bone formation indices reported in this study (OS/BS, O.Th, and OV/BV) are comparable to values published for the iliac-crest biopsy[17,25] and for the vertebral body.[1] We found these indices to be subject-dependent, but they did not correlate with any of the properties of the collagenous matrix, particularly not to the immature/mature cross-link ratio. The basis of the correlation of bone microarchitecture and pyrrole/HP cross-link presents us with a challenging question. The first step is to explore the following problem: Why would an individual subject display a thick and simple microarchitecture, whereas another has a complex thin microarchitecture? Such patterns could be constitutive: after childhood, an individual subject may have a given architecture like any other physical characteristic. There is actually no data to support this hypothesis. Alternatively, the pattern may result from slight but continuous differences in the type of remodeling (during decades). For example, depending on the location or depth of the resorption cavity the osteoclasts[9] may progressively disconnect and simplify the structure.[22] The mechanical feedback may induce a compensatory relative thickening of each element.[8,14]

Formation of pyrrole rather than pyridinoline depends on reduced lysine hydroxylation, including both specific triple helical lysine and telopeptide lysine. Furthermore, the pyrrole cross-links predominate at the amino-terminus of the molecule, whereas the pyridinoline predominate at the carboxy-terminus, indicating a further specificity of lysine hydroxylase.[6,10] Recent isolation of tissue-specific isoenzymes[3,15,27] suggests that each of these lysyl hydroxylases may be specific for each location.

Certainly the cross-linking of collagen affects the susceptibility of fibers to proteolysis.[34] However, it is debatable as to whether the different mature cross-links influence the ability of the proteolytic enzymes from the osteoclast to degrade the fiber. Nevertheless, it is conceivable that the presence of the pyrrole cross-link (instead of HP) may affect the rate of catabolism of bone collagen by metalloproteinases (MMPs) and cysteine proteinases.[26]

All measurements performed herein were made on adult human bone and we chose a skeletal site, the vertebral body, where fractures have a very high frequency.[15] However, as in all studies on humans, there are certain limitations. Although the analyses were carried out on 68 cylindrical samples, these important results now need to be carried out using larger numbers of subjects. A second point, to be taken into account in the future, albeit less important, involves the length of bed-rest prior to death. Although the autopsy subjects were selected to eliminate bone or metastatic disease, prolonged bed-rest may have influenced the osteoid indices. However, the major emphasis of this study was on the collagenous matrix of the microarchitecture, which takes years to construct.[23]

This study is the first in which there is an indication of a link between the structural organization of the trabeculae and the nature of the tissue that composes these trabeculae, in terms of the cross-link stabilizing the collagen fiber.

The biochemical stability and structure of the collagen fibers may therefore be an important factor qualitatively affecting cancellous bone turnover and, hence, its final microarchitecture.

76   X. Banse et al.
      Cross-links and morphometry

Bone Vol. 31, No. 1
July 2002:70–76

References

1. Alexiades, M. M., Boachie-Adjei, O., and Vigorita, V. J. Histomorphometric analysis of vertebral and iliac crest bone samples. A correlated study. Spine 15:286–288; 1990.

2. Bailey, A. J., Sims, T. J., Ebbesen, E. N., Mansell, J. P., Thomsen, J. S., and Mosekilde, L. Age-related changes in the biochemical properties of human cancellous bone collagen: Relationship to bone strength. Calcif Tissue Int 65:203–210; 1999.

3. Bank, R. A., Robins, S. P., Wijmenga, C., Breslau-Siderius, L. J., Bardoel, A. F., van der Sluijs, H. A., Pruijs, H. E., and TeKoppele, J. M. Defective collagen crosslinking in bone, but not in ligament or cartilage, in Bruck syndrome: Indications for a bone-specific telopeptide lysyl hydroxylase on chromosome 17. Proc Natl Acad Sci USA 96:1054–1058; 1999.

4. Banse, X., Devogelaer, J. P., and Grynpas, M. Patient specific micro-architecture of the vertebral cancellous bone: A pQCT and histological study. Bone. In press.

5. Banse, X., Devogelaer, J. P., Munting, E., Delloye, C., Cornu, O., and Grynpas, M. D. Inhomogeneity of human vertebral cancellous bone. Systematic density and structure patterns inside the vertebral body. Bone 28:563–571; 2001.

6. Brady, J. D. and Robins, S. P. Structural characterization of pyrrolic cross-links in collagen using a biotinylated Ehrlich's reagent. J Biol Chem 276:18812–18818; 2001.

7. Compston, J. E., Mellish, R. W., and Garrahan, N. J. Age-related changes in iliac crest trabecular microanatomic bone structure in man. Bone 8:289–292; 1987.

8. Dempster, D. W. The contribution of trabecular architecture to cancellous bone quality. J Bone Miner Res 15:20–23; 2000.

9. Eriksen, E. F., Mosekilde, L., and Melsen, F. Trabecular bone resorption depth decreases with age: Differences between normal males and females. Bone 6:141–146; 1985.

10. Eyre, D. R., Dickson, I. R., and Van-Ness, K. Collagen cross-linking in human bone and articular cartilage. Age-related changes in the content of mature hydroxypyridinium residues. Biochem J 252:495–500; 1988.

11. Ghosh, D., Deisher, T. A., and Ellsworth, J. L. Statistical methods for analyzing repeated measures. J Pharmacol Toxicol Meth 42:157–162; 1999.

12. Gordon, C. L., Lang, T. F., Augat, P., and Genant, H. K. Image-based assessment of spinal trabecular bone structure from high-resolution CT images. Osteopor Int 8:317–325; 1998.

13. Grant, R. A. Estimation of hydroxyproline by the AutoAnalyzer. J Clin Pathol 18:686; 1965.

14. Huiskes, R., Ruimerman, R., van Lenthe, G. H., and Janssen, J. D. Effects of mechanical forces on maintenance and adaptation of form in trabecular bone. Nature 405:704–706; 2000.

15. Jacobsen, S. J., Cooper, C., Gottlieb, M. S., Goldberg, J., Yahnke, D. P., and Melton, L. J. Hospitalization with vertebral fracture among the aged: A national population-based study, 1986–1989. Epidemiology 3:515–518; 1992.

16. Jiang, Y., Zhao, J., Augat, P., Ouyang, X., Lu, Y., Majumdar, S., and Genant, H. K. Trabecular bone mineral and calculated structure of human bone specimens scanned by peripheral quantitative computed tomography: Relation to biomechanical properties. J Bone Miner Res 13:1783–1790; 1998.

17. Kimmel, D. B., Recker, R. R., Gallagher, J. C., Vaswani, A. S., and Aloia, J. F. A comparison of iliac bone histomorphometric data in post-menopausal osteoporotic and normal subjects. Bone Miner 11:217–235; 1990.

18. Kleerekoper, M., Villanueva, A. R., Stanciu, J., Rao, D. S., and Parfitt, A. M. The role of three-dimensional trabecular microstructure in the pathogenesis of vertebral compression fractures. Calcif Tissue Int 37:594–597; 1985.

19. Knott, L. and Bailey, A. J. Collagen cross-links in mineralizing tissues: A review of their chemistry, function, and clinical relevance. Bone 22:181–187; 1998.

20. Knott, L., Tarlton, J. F., and Bailey, A. J. Chemistry of collagen cross-linking: Biochemical changes in collagen during the partial mineralization of turkey leg tendon. Biochem J 322:535–542; 1997.

21. Kuypers, R., Tyler, M., Kurth, L. B., Jenkins, I. D., and Horgan, D. J. Identification of the loci of the collagen-associated Ehrlich chromogen in type I collagen confirms its role as a trivalent cross-link. Biochem J 283:129–136; 1992.

22. Mosekilde, L. Consequences of the remodelling process for vertebral trabecular bone structure: A scanning electron microscopy study (uncoupling of unloaded structures). Bone Miner 10:13–35; 1990.

23. Parfitt, A. M. Bone remodeling: Relationship to the amount and structure of bone, and the pathogenesis and prevention of fractures. In: Riggs, B. L. and Melton, L. J., eds. Osteoporosis: Etiology, Diagnosis, and Management. New York: Raven; 45–93; 1988.

24. Parfitt, A. M., Drezner, M. K., Glorieux, F. H., Kanis, J. A., Malluche, H., Meunier, P. J., Ott, S. M., and Recker, R. R. Bone histomorphometry: Standardization of nomenclature, symbols, and units. Report of the ASBMR Histomorphometry Nomenclature Committee. J Bone Miner Res 2:595–610; 1987.

25. Parfitt, A. M., Han, Z. H., Palnitkar, S., Rao, D. S., Shih, M. S., and Nelson, D. Effects of ethnicity and age or menopause on osteoblast function, bone mineralization, and osteoid accumulation in iliac bone. J Bone Miner Res 12:1864–1873; 1997.

26. Parikka, V., Lehenkari, P., Sassi, M. L., Halleen, J., Risteli, J., Harkonen, P., and Vaananen, H. K. Estrogen reduces the depth of resorption pits by disturbing the organic bone matrix degradation activity of mature osteoclasts. Endocrinology 142:5371–5378; 2001.

27. Passoja, K., Rautavuoma, K., Ala-Kokko, L., Kosonen, T., and Kivirikko, K. I. Cloning and characterization of a third human lysyl hydroxylase isoform. Proc Natl Acad Sci USA 95:10482–10486; 1998.

28. Pocock, S. J., Geller, N. L., and Tsiatis, A. A. The analysis of multiple endpoints in clinical trials. Biometrics 43:487–498; 1987.

29. Robins, S. P. Fibrillogenesis and maturation of collagens. In: Seibel, M. J., Robins, S. P., and Bilezikian, J. P., eds. Dynamics of Bone and Cartilage Metabolism. San Diego, CA: Academic; 31–42; 1999.

30. Schenk, R. K., Olah, A. J., and Herrmann, W. Preparation of calcified tissues for light microscopy. In: Dickson, G. R., ed. Methods in Calcified Tissue Preparation. New York: Elsevier; 1–56; 1984.

31. Scott, J. E., Hughes, E. W., and Shuttleworth, A. A collagen-associated Ehrlich chromogen: A pyrrolic crosslink. Biosci Rep 1:611–618; 1981.

32. Sims, T. J., Avery, N. C., and Bailey, A. J. Quantitative determination of collagen cross-links. In: Streuhli, C. and Grant, M. E., eds. Methods in Molecular Biology, Vol. 139. New York: Humana; 11–26; 2000.

33. Sims, T. J. and Bailey, A. J. Quantitative analysis of collagen and elastin cross-links using a single-column system. J Chromatogr 582:49–55; 1992.

34. Vater, C. A., Harris, E. D. J., and Siegel, R. C. Native cross-links in collagen fibrils induce resistance to human synovial collagenase. Biochem J 181:639–645; 1979.

35. Vesterby, A. Star volume of marrow space and trabeculae in iliac crest: Sampling procedure and correlation to star volume of first lumbar vertebra. Bone 11:149–155; 1990.